NASA Technical Memorandum 86433
USAAVSCOM Technical Memorandum 85-B-3

COMPARISONS OF VARIOUS CONFIGURATIONS OF THE EDGE DELAMINATION TEST FOR INTERLAMINAR FRACTURE TOUGHNESS

T. Kevin O'Brien, N. J. Johnston,
I. S. Raju, D. H. Morris, and
R. A. Simonds

July 1985

National Aeronautics and
Space Administration
Langley Research Center
Hampton, Virginia 23665

SUMMARY

Various configurations of Edge Delamination Tension (EDT) test specimens were manufactured and tested to assess the usefulness of each configuration for measuring interlaminar fracture toughness. Tests were performed on both brittle (T300/5208) and toughened-matrix (T300/BP907) graphite reinforced composite laminates. The mixed-mode interlaminar fracture toughness, G_c, was measured during tension tests of $(30/-30_2/30/90_n)_s$, n=1 or 2, $(35/-35/0/90)_s$, and $(35/0/-35/90)_s$ layups designed to delaminate at low tensile strains. Laminates were made without inserts so that delaminations would form naturally between the central 90° plies and the adjacent angle plies. Laminates were also made with Teflon inserts implanted between the 90° plies and the adjacent angle (θ) plies at the straight edge to obtain a planar fracture surface. In addition, mode I interlaminar tension fracture toughness, G_{Ic}, was measured from laminates with the same layups but with inserts in the midplane, between the central 90° plies, at the straight edge. All of the EDT configurations were useful for ranking the delamination resistance of composites with different matrix resins. Furthermore, the variety of layups and configurations available yield interlaminar fracture toughness measurements, both pure mode I and mixed mode, needed to generate delamination failure criteria.

The influence of insert thickness and location, and coupon size on G_c values were evaluated. For toughened-matrix composites, laminates with 1.5-mil thick inserts yielded interlaminar fracture toughness numbers consistent with data generated from laminates without inserts. Coupons of various sizes yielded similar G_c values. The influence of residual thermal and moisture stresses on calculated strain energy release rate for edge delamination was also reviewed. Edge delamination data may be used to quantify the relative influence of

residual thermal and moisture stresses on interlaminar fracture for different composite materials.

NOMENCLATURE

Δa	Finite element size at delamination front
E	Axial modulus
E_{LAM}	Laminate modulus
E^*	Modulus of laminate completely delaminated along one or more interfaces
E_{11}, E_{22}	Lamina moduli
G_{12}	Lamina shear moduli
G	Strain energy release rate
G_I, G_{II}, G_{III}	Strain energy release rate components due to opening, sliding shear, and tearing shear fracture modes
G^M, G^{M+T}, G^{M+T+H}	Strain energy release rate due to mechanical, mechanical plus thermal, and mechanical plus thermal plus hygroscopic loads
G_c	Critical strain energy release rate for delamination onset
G_{Ic}	Critical mode I strain energy release rate for delamination onset
ΔH	Percentage moisture weight gain
h	ply thickness
N	Number of plies
N_x, N_y, N_{xy}	In-plane stress resultants

M_x, M_y, M_{xy} Moment resultants

$[Q]$ Transformed reduced stiffness matrix

ΔT Temperature difference between stress-free temperature and test temperature

t laminate thickness

t_A Thickness of adhesive bond

u Strain energy density

$\varepsilon_x, \varepsilon_y, \gamma_{xy}$ In-plane strains

$\kappa_x, \kappa_y, \kappa_{xy}$ Out-of-plane curvatures

ν_{12} Lamina Poisson's ratio

σ Stress

θ Fiber orientation angle

INTRODUCTION

A simple tension test was proposed for measuring the mixed-mode interlaminar fracture toughness of composites [1-5]. In this test,laminates are loaded in tension to develop high interlaminar tensile and shear stresses at the straight edge causing delamination. For these laminates, a noticeable change in the linear load-deflection curve occurs at the onset of edge delamination. The strain at delamination onset is substituted into a closed form equation for strain energy release rate, G, to obtain the critical value, G_c, for edge delamination. This G_c value is a measure of the interlaminar fracture toughness of the composite material. Finite element analyses are performed to obtain the contribution of the crack-opening, G_I, sliding-shear, G_{II}, and tearing-shear, G_{III}, fracture modes to the total strain energy release rate.

The edge delamination tension (EDT) test has been used to rank the relative delamination resistance of composites with brittle and toughened-resin matrices, and determine their fracture mode dependence. However, the accuracy of interlaminar fracture toughness measurements generated from such tests has been questioned [6]. Self-similarity of delamination growth, accuracy of the finite element analysis of mixed-mode ratio ratios, and the influence of residual thermal and moisture stresses on critical strain energy release rates, G_c, are some of the concerns that have been raised. Recently, a pure mode I version of the EDT test, with Teflon inserts embedded in the midplane at the straight edge, was proposed to overcome some of these concerns [7].

This paper will examine interpretation of data for three configurations of the EDT test, one without inserts, one with midplane inserts, and one with inserts at the θ/90 interfaces. Four different layups were tested: $(30,-30_2,30,90_n)_s$, n=1,2, $(35,-35,0,90)_s$, and $(35/0/-35/90)_s$. These layups were

designed to yield the lowest delamination onset strain to measure a given G_c [4]. Laminates were tested in the three configurations: (1) the pure mode-I configuration with mid-plane inserts, (2) a mixed-mode configuration with inserts at the interface between the central 90° plies and the adjacent angle plies, and (3) the original mixed-mode configuration where delaminations form naturally at the θ/90 interfaces. Data generated from EDT tests with different coupon sizes and insert thicknesses were compared for composites with graphite fibers (Thornel T300)* in both brittle (Narmco 5208)* and tough (Cycom BP907)* matrix resins. The accuracy of finite element analysis of mixed-mode ratios and the significance of residual thermal and moisture stresses to strain energy release rates were also addressed.

---

*Use of Manufacturer's trade name does not constitute endorsement, either expressed or implied, by NASA or AVSCOM.

MATERIALS

Composite panels of two graphite epoxy materials; Thornel 300 (T300) fibers in Narmco 5208 matrix and T300 fibers in American Cyanamid BP907 matrix, were fabricated. Table 1 lists the basic lamina properties (E_{11},E_{22},G_{12},ν_{12}) measured for these two materials using the procedure outlined in reference 2. Panels were made with the following layups: $(30/-30_2/30/90_n)_s$, where n=1 or 2, $(35/-35/0/90)_s$, and $(35/0/-35/90)_s$. Thin strips of Teflon were inserted at selected locations in each panel using a template. As shown in figure 1, panels were constructed so that coupons with and without inserts were cut from the same panel. The Teflon strips were either 1.5 or 3.5-mils thick, and were placed either at a single θ/90 interface or at the midplane between the two central ninety degree plies. Coupons were cut from the panels with inserts extending either throughout the width, for determining laminate modulus with the interface completely delaminated, or with inserts extending partially through the width from both edges, for measuring interlaminar fracture toughness. Table 2 lists the five coupon sizes that were tested. Unless otherwise specified, five inch long by one inch wide (size E) coupons were tested.

TEST PROCEDURE

Coupons were loaded in tension, through friction grips, in either a screw-driven or hydraulic machine at a relatively slow crosshead speed. Tests were conducted under ambient laboratory conditions, i.e. at a nominal room temperature of 70°F and a relative humidity of 60%. In most cases, a minimum of five replicate tests were performed for each laminate orientation. Longitudinal strain was measured using extensometers, either a single clip-gage or a pair of direct current differential transducers (DCDT's) mounted on the centers of the front and back faces of the coupon. Table 2 lists the extensometer gage lengths for the various specimen sizes tested. Load and strain were continuously monitored and recorded on an X-Y recorder. Coupons without inserts were loaded until delaminations formed on the edge and the corresponding abrupt jump in the load deflection curve was observed [1-5]. Coupons with inserts extending partially through the width from either edge were loaded until a noticeable change in slope or non-linearity was observed in the load-deflection curve. A zinc-iodide solution was injected in the delaminated interface, and an X-ray radiograph was taken to confirm that a delamination had extended from the Teflon insert. Coupons with inserts extending throughout the laminate width were loaded until a load deflection curve was obtained for measuring laminate modulus with the interface delaminated throughout.

ANALYSIS

Laminated Plate Theory

The interlaminar fracture toughness ,G_c, of a composite laminate is the critical value of the strain energy release rate, G, required to grow a delamination. A closed-form equation was derived for the mixed-mode strain energy release rate for edge delamination growth in a composite laminate [1]. This equation

$$G = \frac{\varepsilon^2 t}{2} (E_{LAM} - E^*) \qquad (1)$$

where ε = nominal tensile strain

t = laminate thickness

E_{LAM} = laminate modulus

E^* = modulus of a laminate completely delaminated along one or more interfaces

is independent of delamination size. The strain energy release rate depends on the laminate layup and the location of the delaminated interface, which determines ($E_{LAM} - E^*$). If the lamina properties are known, then E_{LAM} and E^* can be calculated from laminated plate theory and the rule of mixtures [1-5]. The $(30/-30_2/30/90_n)_s$ layups delaminate at the 30/90 interfaces.

As outlined in ref.[1], after delamination these layups are modeled as three sublaminates, two $(30/-30)_{2S}$ and one $(90)_{2n}$ laminate, loaded in parallel to account for the loss in transverse contraction as delaminations grow under an applied strain. Thus,

$$E^* = \frac{8E_{(30/-30)} + 2nE_{(90)}}{8+2n} \qquad (2)$$

Where $E_{(90)}$ is equal to E_{22}, and $E_{(30/-30)}$ can be calculated either from laminated plate theory or measured from a tensile test of a $(30/-30)_s$ laminate [1-5]. The $(35/-35/0/90)_s$ and $(35/0/-35/90)_s$ layups delaminate between the 0/90 and -35/90 interfaces, respectively. After delamination, these laminates are modeled as two $(35/0/-35)_s$ sublaminates and one $(90)_2$ laminate, yielding

$$E^* = \frac{6E_{(35/0/-35)} + 2E_{(90)}}{8} \qquad (3)$$

where $E_{(35/0/-35)}$ may be calculated either from laminated plate theory or measured from a tensile test of a $(35/0/-35)_s$ laminate. However, assuming the sublaminates to be symmetric yields a slightly different axial modulus than if they are modeled as (35/-35/0) and (35/0/-35) asymmetric laminates due to the bending-extension coupling and twist-extension coupling present in these two asymmetric layups, respectively. The axial modulus of an asymmetric layup may be calculated from laminated plate theory by assuming N_y, N_{xy}, κ_x, M_y, and κ_{xy} are all zero for a constant ε_x [8,9,10]. This technique allows for a non-zero κ_y and yields a slightly different axial modulus for the asymmetric configuration than for the symmetric configuration.

Table 3 compares the axial modulus calculated from laminated plate theory for the (35/-35/0) and (35/0/-35) sublaminates for both the symmetric and asymmetric configurations using lamina properties from table 1. A small difference in modulus was obtained for the $(35/-35/0)_T$ layup compared to the $(35/0/-35)_s$ layup, but no significant difference was observed for the $(35/0/-35)_T$ layup.

Because the delaminations that formed naturally (i.e. without artificially implanted inserts) at θ/90 interfaces in all the layups tested wandered from one θ/90 interface to its symmetric counterpart (fig.2a), these laminates were all modeled as a set of three symmetric sublaminates after delamination (fig.2b), [1-5]. However, for the laminates that contained Teflon inserts in one θ/90 interface (fig.2c), the laminates were modeled as two asymmetric sublaminates after delamination. Hence, the equations for the delaminated modulus ,E^*, for the $(30/-30_2/30/90_n)_s$, $(35/-35/0/90)_s$, and $(35/0/-35/90)_s$ layups become

$$E^* = \frac{4E_{(30/-30)_s} + (4+2n)\, E_{(30/-30_2/30/90_{2n})_T}}{8+2n} \qquad (4)$$

$$E^* = \frac{3E_{(35/-35/0)_T} + 5E_{(35/-35/0/90_2)_T}}{8} \qquad (5)$$

$$E^* = \frac{3E_{(35/0/-35)_T} + 5E_{(35/0/-35/90_2)_T}}{8} \qquad (6)$$

respectively. The asymmetric sublaminate moduli in equations 4-6 were calculated using lamina properties from table 1 and are listed in table 3. Table 4 compares the delaminated modulus, E^*, calculated for the natural delamination to E^* values calculated for the single artificially-delaminated θ/90 interface. The differences among E^* values, and hence the corresponding differences among G values from equation (1), illustrate that for the natural delamination case the delamination is driven only by a mismatch in transverse (Poisson) contraction between the sublaminates, but for the artificially delaminated case, the delamination is driven by a combination of Poisson mismatch and the curvature assumed by the asymmetric sublaminates before the delamination grows from the insert.

If the insert is placed at the mid-plane between the two central 90°plies (fig.2d), as was proposed in reference [7], then no Poisson mismatch results, and the delamination is driven entirely by the curvature assumed by the asymmetric sublaminates before the delamination grows from the insert. For this mid-plane delamination case, the delaminated moduli of the $(30/-30_2/30/90_n)_s$, $(35/-35/0/90)_s$, and $(35/0/-35/90)_S$ layups become

$$E^* = E_{(30/-30_2/30/90_n)_T} \tag{7}$$

$$E^* = E_{(35/-35/0/90)_T} \tag{8}$$

$$E^* = E_{(35/0/-35/90)_T} \tag{9}$$

respectively. The asymmetric moduli in eqs.7-9 were calculated using lamina properties from table 1 and listed in table 4 as E^* for a midplane (90/90 interface) insert. Because these midplane delaminations are driven entirely by asymmetric sublaminate curvature with no Poisson mismatch, the delamination is purely an opening mode-I fracture. Therefore, for midplane delamination, eq.1 becomes

$$G_I = \frac{\varepsilon^2 t}{2} (E_{LAM} - E^*) \tag{10}$$

where E^* is calculated from one of equations 7-9, for the particular layup tested.

Recently, an analysis was developed that incorporates the influence of residual thermal and moisture stresses to the strain energy release rate for

edge delamination [10]. This analysis yielded the following equation for the total strain energy release rate

$$G = t_{LAM}u_{LAM} - t_{SUB}u_{SUB} - t_{90}u_{90} \qquad (11)$$

where t is the thickness and u is the strain energy density of the original laminate (LAM), the sublaminates (SUB) ,and the ninety degree plies (90). The strain energy density is defined as

$$u = \frac{1}{2N} \sum_{k=1}^{N} \{\varepsilon\}_k' \{\sigma\}_k \qquad (12)$$

where N is the number of plies, and $\{\varepsilon\}_k'$ is the transpose of the total strain vector for the kth ply, which includes contributions from mechanical loading, thermal gradients (ΔT), and hygroscopic (moisture) percentage weight gain (ΔH). The stress vector for the kth ply in eq.12 is given by

$$\{\sigma\}_k = [\bar{Q}]_k \{\varepsilon\}_k \qquad (13)$$

where $[\bar{Q}]_k$ is the transformed reduced stiffness matrix of the kth ply as defined in laminated plate theory. Therefore, equation 11 requires a ply-by-ply evaluation of the strain energy density in the laminated and delaminated regions to account for the biaxial thermal and moisture stresses present in the laminate.

Figure 3 shows the influence of residual thermal and moisture stresses on G for edge delamination in the -30/90 interfaces of the eleven-ply $(30/-30/30/-30/90/\overline{90})_s$ laminate with an applied mechanical strain of 0.01 and ΔT = -280°F. As shown on the ordinate, the strain energy release rate due to

mechanical loading only, G^M, calculated from eq.11 is identical to G calculated from eq.1. However, if the residual thermal strain is included, the strain energy release rate, G^{M+T}, is higher than G^M for the same applied mechanical strain. If the laminate also absorbs moisture, the residual thermal stresses are relaxed and the strain energy release rate, G^{M+T+H}, decreases depending on the percentage of moisture weight gain, ΔH. For the case shown in fig.3, the residual thermal stresses are completely relaxed after a moisture weight gain of approximately 0.7% where G^{M+T+H} is equal to G^M. Epoxy matrix composites may absorb nearly this much water from the ambient laboratory air in a matter of weeks [10]. Therefore, the influence of residual thermal stresses may be relatively small at ambient conditions, but may become more significant under dry or water-saturated conditions. Furthermore, composites that are manufactured at higher temperatures but absorb very little moisture may require that thermal and moisture effects be included in the G analysis for edge delamination. However, the relative contribution of residual thermal and moisture stresses to G is smaller for toughened-matrix composites that delaminate at high strains because a large mechanical strain at delamination onset has a much greater contribution to the strain energy released than ΔT or ΔH.

The tests in this study were conducted on graphite epoxy materials in the ambient laboratory environment described earlier. Therefore, the influence of residual thermal and moisture stresses were not included in the data reduction for these tests.

Finite Element Analysis

A quasi-three dimensional finite element analysis was performed with the virtual-crack-extension technique to determine the G_I, G_{II}, and G_{III} components

of the total strain energy release rate for several configurations of the edge delamination test [1-5]. In reference [1], the G_I,G_{II}, and G_{III} components were calcuated for an eleven-ply $(30/-30/30/-30/90/\overline{90})_s$ layup that delaminated in the -30/90 interfaces. The G_{III} component was negligible for this layup. The delamination growth was modeled for four different initial delamination sizes. The results indicated that the G_I/G_{II} ratio varied with delamination size; however, the finite element mesh used in ref.[1] was very coarse for the longest delamination sizes modeled. Subsequent finite element analyses of this layup [2], and other layups [4,5], were performed with a single mesh refinement for all delamination lengths. These analyses indicated that the G_I and G_{II} components were independent of delamination length.

Recently, an anisotropic elasticity solution and singular hybrid finite element formulation were employed to analyse the strain energy release rate components for edge delamination [11]. Figure 4 compares the nondimensionalized strain energy release rate components calculated for delamination in the -35/90 interfaces of a $(0/35/-35/90)_s$ laminate using both the displacement-based, eight-noded square, parabolic finite elements and the singular hybrid element at the delamination front. Both analyses were performed with several different mesh refinements, and the results have been plotted as a function of element size at the delamination front, Δa, normalized by ply thickness, h. Between $0.18 < \Delta a/h < 0.55$, the singular hybrid element yields constant G_I and G_{II} values. However in reference [11], the singular hybrid analysis yielded variable G_I and G_{II} values for singularity element sizes $\Delta a/h < 0.18$, and for $\Delta a/h > 0.55$. The reasons for these variations are the following. First, for $\Delta a/h < 0.18$, the neighboring regular eight-noded elements are also subjected to the singular stress field. Thus, the crack tip element is too small. Second, for $\Delta a/h > 0.55$, the crack tip singular elements are required to capture both the singular and

far-field components, which the singular element is unable to handle. Thus the crack tip element is too large. However, when the size of the singular element is $0.18 < \Delta a/h < 0.55$, the element is not subjected to these extreme requirements and is able to delineate the stress field accurately and yield accurate G_I and G_{II} values. Therefore, the singular hybrid analysis with mesh refinements in this range may be used as a bench mark solution to compare to other solutions.

In contrast to the results for the singular hybrid element, the G_I and G_{II} values calculated with the eight-noded displacement-based element at the delamination front vary continuously with $\Delta a/h$. Therefore, a converged solution is never obtained for this element using the virtual-crack-extension technique. However, if an element size of $\Delta a/h=0.25$ is used, the G components calculated with the eight-noded element agree fairly well with the singular-hybrid element results. Hence, four square elements through the ply thickness, with dimensions $\Delta a/h = 0.25$, appear to be a good choice for the displacement-based finite element mesh at the delamination front. Table 5 lists the ratio of G_I to the total G calculated for the four layups tested in this study with either natural delamination, where both $\theta/90$ interface delaminations are modeled, or for a single $\theta/90$ delamination growing from an insert. These G_I/G ratios were calculated using the displacement-based finite element analysis with the suggested mesh refinement. The total G consisted of G_I and G_{II} only since the calculated G_{III} component was negligible for each case.

RESULTS

Test data were compared for laminates with various insert thicknesses, insert locations, and coupon sizes to indentify if these differences in configuration influenced interlaminar fracture toughness measurement. Because previous studies using the edge delamination test on graphite epoxy composites indicated that the G_I component alone may control the onset of delamination, the G_I components of the measured G_c for different layups were compared first [4,5]. In addition, G_c measurements were plotted as a function of the G_I and G_{II} components assuming a linear failure criterion.

Variation in G_c with insert thickness

Because the interlaminar fracture toughness is measured at the onset of delamination from the insert embedded at the straight edge, the thickness of the insert will determine the relative sharpness of the delamination front. If the insert is too thick, the delamination may behave as if the crack tip was blunted and had a finite notch root radius. This blunted crack would yield higher apparent toughness values than a sharp crack. Therefore, EDT coupons were made with two different insert thicknesses, and data were compared to adhesive bond toughness data with comparable bond thicknesses to determine if interlaminar fracture toughness values could be obtained from coupons with inserts.

Figure 5 compares interlaminar fracture toughness measurements for $(30/-30_2/30/90_2)_s$ laminates made of T300/5208 and T300/BP907. Tests were conducted on laminates with 3.5 and 1.5-mil inserts at the midplane, and on laminates without inserts. All three configurations showed the improved

toughness of the T300/BP907 compared to the T300/5208 material. For both materials, the laminates with the thicker inserts yielded higher apparent toughness values than the laminates with the thinner inserts.

As illustrated in fig.6, these results may be compared to fracture toughness measurements of adhesive bonds assuming that the resin pocket that forms at the end of the insert is analagous to an adhesive bond with a thickness, t_A, equal to the insert thickness. Previous work on adhesive bond fracture indicated that the bond thickness must be below a certain value to achieve a realistic fracture toughness measurement [12]. Figure 7 shows fracture toughness measurements determined from double cantilever beam (DCB) adhesive bond tests, with BP907 as the adhesive, as a function of bond thickness. The data indicate that fracture toughness is constant for bond thicknesses below 2.5 mils. For bond thicknesses greater than 2.5 mils, fracture toughness measurements are unrealistically high due to the relaxed constraint on the resin allowing greater localized plastic deformation near the crack tip. Using the adhesive bond analogy, the G_{Ic} results shown in fig.5 for T300/BP907 EDT tests may be artificially elevated for the laminates with 3.5-mil inserts, but G_{Ic} values for laminates with 1.5-mil inserts should be representative of G_{Ic} for delamination growth between plies.

Figure 5 also shows G_c results for laminates without inserts (open symbols) and their G_I components calculated from finite element analysis (table 5). For the T300/BP907, the G_I component of the natural delamination mixed-mode test agrees well with the G_{Ic} measurement from the laminate with the 1.5-mil insert and G_{Ic} measurements from DCB tests on thin adhesive bonds (fig.7) [12].

For the T300/5208 laminates, the G_I component of the natural delamination mixed-mode test was higher than the G_{Ic} measurements from laminates with both the 1.5-mil and 3.5-mil midplane inserts. However, these natural delamination G_c

values were higher than G_c values measured previously on eleven-ply layups [1], and they had considerably more scatter than the G_{Ic} measurements, which may indicate that extensive matrix cracking may have been present in the four central 90-degree plies before delamination occurred [4]. Therfore, these experiments were repeated on ten-ply $(30/-30_2/30/90)_s$ laminates that were less likely to experience extensive matrix cracking before delamination because of the reduced number of ninety-degree plies.

Figure 8 shows results obtained from the ten-ply T300/5208 laminates. The total G_c measurements were slightly lower and had less scatter than results for the twelve-ply laminate, but the G_I component still exceeded the G_{Ic} values obtained from the two midplane insert tests. The trend of higher interlaminar fracture toughness for the natural delamination compared to the fracture toughness of the thin adhesive bonds simulated by the teflon inserts is consistent with the trends noted when comparing neat resin G_{Ic} fracture toughness values for brittle resins to interlaminar G_{Ic} values as measured by composite double cantilever beam (DCB) tests [13]. For example, figure 9 shows the correlation between neat resin G_{Ic} and composite G_{Ic} for a variety of resin matrices. For the tougher resins, neat resin G_{Ic} exceeds composite G_{Ic} due to the large plastic zones that form in neat resin fracture tests. However, for the brittle resin matrices, neat resin G_{Ic} is less than G_{Ic} for the composite. Apparently, the close proximity of the fibers in the composite, which is analagous to a very thin bond line, does not significantly lower toughness by increasing constraint for the brittle resin, but may actually increase the toughness due to the interaction of the crack front with the fibers creating more plastic flow locally at the fibers than was observed in neat resin fracture tests [14].

All subsequant test data reported was generated with the 1.5 mil inserts and compared to data generated from coupons without inserts.

Variation in G_c with insert location

Figure 10 compares the G_{Ic} values for midplane delamination of the T300/BP907 ten-ply $(30/-30_2/30/90)_s$ layup with the G_I components of G_c for the natural mixed-mode delamination, and for mixed-mode delamination from inserts in a single 30/90 interface. These G_I values are in excellent agreement. Therefore, all three configurations of this 30/90 layup yield similar results for the T300/BP907 toughened-matrix composite.

Variation in G_c with coupon size

Mixed mode delamination tests where conducted on $(35/-35/0/90)_s$ T300/5208 laminates with and without inserts, and on T300/BP907 laminates without inserts, using five different coupon sizes (table 2). Figure 11 compares G_c measurements for the five coupon sizes. The variation in mean values of G_c measurements for the T300/5208 and T300/BP907 laminates without inserts was small compared to the scatter in the data for each coupon size. However, for the T300/5208 laminates with inserts, the coupons with ten inch gage lengths appeared to yield slightly lower G_c values than coupons with five inch gage lengths. This difference may be attributable to the contribution of curvature to delamination growth discussed previously. The uniform κ_y curvature in the asymmetric sublaminates may be less extensive in the shorter specimens because of the smaller distance between the grips in the shorter coupons.

Variation in G_c with Layup

Figure 12 compares G_c and G_{Ic} data for $(35/-35/0/90)_s$ and $(35/0/-35/90)_s$ T300/5208 laminates with no inserts, with midplane inserts, and with inserts at a single θ/90 interface. For the mixed-mode configurations, the G_c values for the two layups do not agree. Table 5 shows that the G_I/G ratios for these two layups are different. Although the two layups have different mode I percentages, fig.12 indicates that the G_I components for delamination onset from the insert in the θ/90 interface are nearly identical for both layups. The G_{Ic} values from coupons of the two layups containing midplane inserts also agree. However, the G_{Ic} values from laminates with midplane inserts were lower than the G_I components of G_c for laminates with θ/90 interface inserts. As noted earlier for the 30/90 layup, for the brittle 5208 matrix composite the toughness measurements from laminates with inserts are lower than the measurements from natural delamination.

Although the data generated in this study indicates that the G_I component is responsible for delamination growth even under mixed-mode loading, the criterion for mixed-mode delamination may be generally expressed as a failure envlope defined by the polynomial

$$\left(\frac{G_I}{G_{Ic}}\right)^m + \left(\frac{G_{II}}{G_{IIc}}\right)^n = 1 \qquad (14)$$

In reference [15] interlaminar fracture data in the literature was plotted and indicated that a linear failure criterion, where m=1 and n=1, provided the best fit to the data. Figures 13 and 14 show similar plots for T300/5208 and for T300/BP907 using the data generated in this study along with edge delamination

data for T300/BP907 from ref.[16], and G_{IIc} data from End-notched flexure tests [17]. These plots also indicate that a linear failure criterion may be appropriate, however data from tests with other G_I/G_{II} ratios are needed to accurately determine the shape of the failure envelope. Because the G_{IIc} values are nearly an order of magnitude larger than the G_{Ic} values for these two materials, the failure envelope is almost horizontal over the range of G_I/G_{II} ratios tested. Therefore, even if delamination failure is governed by a linear failure criterion as depected in figures 13 and 14, the failure appears to be controlled by the G_I component alone when the data is plotted as shown in figures 5,10, and 12.

DISCUSSION

This discussion will summerize some of the advantages and disadvantages of the the edge delamination tension (EDT) test configurations with and without inserts. Some advantages and disadvantages are common to both configurations. The EDT test involves a simple loading, does not require a measurement of delamination size, may be conducted on a variety of layups to provide a range of mixed-mode ratios, yields data consistent with other interlaminar fracture tests, and provides a ranking of the relative interlaminar fracture toughness of different composite materials. However, for EDT layups with zero-degree plies, G_c measurement is limited by the failure strain of the fibers, whereas for layups without zero degree plies, toughened-matrix composites may exhibit nonlinearity in the load-displacement curve before delamination onset [2,4]. Alternate layup designs such as $(35/-35_2/35/0_2/90)_s$, where the increased laminate thickness reduces the strain required to measure a given G_c, may overcome these limitations. No closed-form elasticity solution exists for edge delamination that yields G_I, G_{II}, and G_{III} for arbitrary layups, however, a singular-hybrid

finite element analysis yields a bench-mark solution for the various G components. The G_c measurements from the EDT test may be influenced by residual thermal and moisture stresses, which can be included in the data reduction but would require measurement of stress free temperature, moisture content, and moisture and thermal coefficients of expansion.

One motivation for including inserts at the edge was to remove the uncertainties in assuming the delaminations that naturally wander from one θ/90 interface to another (fig.2a) can be modeled as three sublaminates loaded in parallel (fig.2b). Although the formation of the pattern shown in fig.2a along the edge is random, once the pattern is formed it remains unchanged as the delamination grows through the laminate width. Therefore the delamination growth through the width is self-similar, and the strain energy release rate associated with this growth is reflected in eq.1, as long as the delaminated modulus, E^*, accurately represents the modulus after the natural delamination has extended through the laminate width. Plots of modulus as a function of delamination size were generated in previous studies and indicated that eqs.2-4 provide a fairly accurate estimate of delaminated laminate modulus [1,18,19]. Inclusion of an insert throughout the laminate width at the appropriate interface, however, provides a direct measure of the delaminated modulus, in addition to providing a single planar delamination front for EDT tests. Therefore, the insert eliminates the need for lamina property measurements and laminate plate theory analysis to determine E^*. However, the EDT tests with inserts have some disadvantages not found in the natural delamination coupons. A template is needed to locate inserts during the layup of the panel, and the insert material may deform during the cure resulting in non-uniform insert thickness in the panel. Non-uniformity of insert thickness may cause uncertaintity in the determination of E^* and G_c. In addition, the deviation from the linear load-displacement curve is not as

abrupt for laminates with inserts. Because the delamination grows from an embedded insert, delamination onset cannot be visually verified. Hence, the delamination onset strain is more difficult to determine in laminates with inserts. Furthermore, because implanted delaminations at one asymmetrically-located interface or at the midplane result in a bending-extension coupling contribution to E^*, G_c measurements may vary slightly with specimen size.

Table 6 summerizes the advantages and disadvantages of the edge delamination test. Most of the concerns about accurate G_c measurement with the EDT test may be overcome by choosing appropriate layups, thicknesses, and coupon sizes, or by implanting inserts at selected interfaces. However, for all the configurations of the edge delamination test, residual thermal and moisture stresses will contribute to the strain energy release rate for edge delamination.

The significance of residual thermal and moisture stresses to strain energy release rates ultimately depends on how these measurements are used. If toughness measurements are used to compare materials for improved delamination resistance, then these thermal and moisture effects become of secondary importance. This is especially true if tests are conducted at room-temperature ambient conditions, and the difference in toughness measurements for different materials is large [3,5]. For example, the seven percent error in G_c calculated in reference [10] due to neglecting thermal and moisture effects for T300/5208 EDT tests is insignificant compared to the ten-fold increase in G_c measured for composites with toughened matrices [3,5]. If, however, these interlaminar toughness measurements are used as delamination failure criteria to predict delamination growth in composite structures of the same material, but with different geometries and loadings, then these thermal and moisture effects may become more significant. Other factors may need to be addressed to accurately

calculate G. For example, assuming a constant ΔT from the cure temperature over which there exists a constant coefficient of thermal expansion may be physically unrealistic. In addition, assuming that the average moisture content of the laminate is representative of the moisture content at the delamination front may also be in error. Some knowledge of the moisture distribution through the laminate may be needed. The detailed information required for carefully conducted laboratory tests may not be available to analyze the strain energy release rate for the delamination growing in the structure. Nevertheless, conducting edge delamination tests where these effects can be quantified, and compared to data from other interlaminar fracture toughness tests where these effects are not present, would help document the relative influence of residual thermal and moisture stresses on the interlaminar fracture of composite materials.

CONCLUSIONS

Edge delamination tension (EDT) tests were performed on both brittle (T300/5208) and toughened-matrix (T300/BP907) graphite reinforced composite laminates designed to delaminate at the straight edge. The mixed-mode interlaminar fracture toughness, G_c, was calculated from straight edge delamination data measured during tension tests of $(30/-30_2/30/90_n)_s$, n=1 or 2, $(35/-35/0/90)_s$, and $(35/0/-35/90)_s$ laminates without inserts, and laminates with inserts at the $\theta/90$ interface. In addition, mode I interlaminar tension fracture toughness, G_{Ic}, was measured from laminates with the same layups but with inserts in the midplane at the straight edge. The influence of insert thickness and location, coupon size, and layup on G_c measurement was evaluated. Based on the results of this study, the following conclusions were reached:

1. All configurations of the EDT test were useful for ranking the delamination resistance of composites with different matrix resins.
2. Strain energy release rate components may be accurately calculated with displacement-based elements, using the virtual-crack-extension technique, if eight-noded square parabolic elements are used at the delamination front with side dimensions equal to one quarter of the ply thickness.
3. For toughened-matrix composites, laminates with 1.5-mil thick inserts yielded interlaminar fracture toughness numbers consistent with data generated from laminates without inserts.
4. Coupons of various sizes yielded similar results.
5. Delamination appeared to be governed by a linear failure criterion relating G_I and G_{II}.

REFERENCES

1. O'Brien,T.K., "Characterization of delamination onset and growth in a Composite Laminate," in Damage in Composite Materials, ASTM STP 775, June, 1982, p.140.
2. O'Brien,T.K., Johnston,N.J., Morris,D.H., and Simonds,R.A., "A Simple Test for the Interlaminar Fracture Toughness of Composites," SAMPE Journal, Vol.18, No.4, July/August 1982, p.8.
3. Johnston,N.J., O'Brien,T.K., Morris,D.H., and Simonds,R.A., "Interlaminar Fracture Toughness of Composites II - Refinement of the Edge Delamination Test and Application to Thermoplastics," Proceedings of the 28th National SAMPE Symposium and Exhibition, Anaheim, California, April, 1983, p.502.

4.O'Brien,T.K., "Mixed-Mode Strain-Energy-Release-Rate Effects on Edge Delamination of Composites," in Effects of Defects in Composite Materials, ASTM STP 836, 1984, p.125.

5.O'Brien,T.K., Johnston,N.J., Morris,D.H., and Simonds,R.A., "Determination of Interlaminar Fracture Toughness and Fracture Mode Dependence of Composites using the Edge Delamination Test," Proceedings of the International Conference on Testing, Evaluation, and Quality Assurance of Composites, University of Surrey, Guildford, England, September, 1983, p.223.

6.Whitney,J.M., Browning,C.E., and Hoogsteden,W., "A Double Cantilever Beam Test for Characterizing Mode I Delamination of Composite Materials," Journal of Reinforced Plastics and Composites, Vol.1, No.4, 1982, p.297.

7.Whitney,J.M., and Knight,M., "A Modified Free-Edge Delamination Specimen," in Delamination and Debonding of Materials, ASTM STP 876, 1985.

8.Ho,T., and Schapery,R.A., "The Effect of Environment on the Mechanical Behavior of AS/3501-6 Graphite Epoxy Material--Phase IV, Naval Air Systems Command (ATC) Report No. R-92000/3CR-9, February, 1983.

9.Whitcomb,J.D., and Raju,I.S., "Analysis of Interlaminar Stresses in Thick Composite Laminates With and Without Edge Delamination," in Delamination and Debonding of Materials, ASTM STP 876, 1985.

10.O'Brien,T.K., Raju,I.S., and Garber,D.P., "Residual Thermal and Moisture Influences on the Strain Energy Release Rate Analysis of Edge Delamination," NASA TM-86437, 1985.

11. Wang,S.S., "The Mechanics of Delamination in Fiber-Reinforced Composite Materials-Part III," NASA CR-177957, 1985.

12. Chai,H., "On the Bond Thickness Effect in Adhesive Joints and its Significance to Composites Mode I Interlaminar Fracture," presented at the Seventh ASTM Conference on Composite Materials: Testing and Design, April, 1984.

13. Hunston,D.L., "Composite Interlaminar Fracture: Effect of Matrix Fracture Energy," Composites Technology Review, Vol.6, No.4, Winter, 1984, p.176.

14. Bascom,W.D.,Boll,D.J.,Fuller,B.,and Phillips,P.,"Fractography of the Interlaminar Fracture of Carbon Fiber Epoxy Composites," Presented at the ASTM Symposium on Toughened Composites, Houston, Texas, March, 1985.

15. Johnson,W.S., and Mangalgari,P.D., "Influence of Resin on Interlaminar Fracture," Presented at the ASTM Symposium on Toughened Composites, Houston, Texas, March, 1985.

16. Adams,D.F.,Zimmerman,R.S., and Odem,E.M., "Determining Frequency and Load Ratio Effect on the Edge Delamination Test in Graphite/Epoxy Composites," Presented at the ASTM Symposium on Toughened Composites, Houston, Texas, March,1985.

17. Murri,G.B. and O'Brien,T.K., "Interlaminar G_{IIc} Evaluation of Toughened-Resin Matrix Composites using the End-Notched Flexure Test," Proceedings of the 26th AIAA/ASME/ASCE/AHS Structures, Structural Dynamics, and Materials Conference, April 1985, Orlando, Florida, pp.197-202.

18. O'Brien,T.K., "The Effect of Delamination on the Tensile Strength of Unnotched, Quasi-isotropic, Graphite/Epoxy Laminates," in Proceedings of the SESA/JSME 1982 Joint Conference on Experimental Mechanics, Hawaii,

Part I, Society for Experimental Stress Analysis, Brookfield, Conn., May, 1982,p.236.

19.O'Brien,T.K., Ryder,J.T., and Crossman,F.W., "Stiffness,Strength, and Fatigue Life Relationships for Composite Laminates," Proceedings of the Seventh Annual Mechanics of Composites Review, Dayton, Ohio, Oct.,1981.

TABLE 1 - Lamina Material Properties

	T300/5208	T300/BP907
E_{11}, Msi	18.2	15.0
E_{22}, Msi	1.23	1.23
G_{12}, Msi	0.832	0.700
ν_{12},	0.292	0.314

TABLE 2 - Specimen Dimensions

Coupon Size	Length, in.	Width, in.	Grip distance, in.	Gage length, in.
A	10	1.5	7	4
B	10	1.0	7	4
C	10	0.5	7	4
D	5	0.5	3	1
E	5	1.0	3	1

TABLE 3 - Influence of Asymmetry on Sublaminate Moduli

	E, Msi	
Layup	T300/5208	T300/BP907
$(35/0/-35)_S$	9.699	8.051
$(35/0/-35)_T$	9.698	8.053
$(35/-35/0)_T$	9.562	7.927
$(35/-35/0/90_2)_T$	6.468	5.436
$(35/0/-35/90_2)_T$	6.664	5.604
$(30/-30)_S$	7.030	5.899
$(30/-30_2/30/90_2)_T$	5.640	4.770
$(30/-30_2/30/90_4)_T$	4.885	4.150

TABLE 4 - Delaminated Modulus, E^*, for different EDT configurations

		Delaminated Modulus, E^*, Msi		
Material	Layup	Natural θ/90	θ/90 insert	90/90 insert
T300/5208	$(30/-30_2/30/90)_s$	5.870	6.196	6.420
	$(30/-30_2/30/90_2)_s$	5.097	5.600	5.640
	$(35/-35/0/90)_s$	7.582	7.628	7.550
	$(35/0/-35/90)_s$	7.582	7.802	7.855
T300/BP907	$(30/-30_2/30/90)_s$	4.965	5.222	5.404
	$(30/-30_2/30/90_2)_s$	4.343	4.733	4.770
	$(35/-35/0/90)_s$	6.346	6.370	6.310
	$(35/0/-35/90)_s$	6.346	6.522	6.570

TABLE 5 - G_I/G calculated from finite element analysis

Layup	G_I/G Single θ/90 Delamination	G_I/G Double θ/90 Delamination
$(30/-30_2/30/90)_s$	0.68	0.64
$(30/-30_2/30/90_2)_s$	0.66	0.64
$(35/-35/0/90)_s$	0.76	0.94
$(35/0/-35/90)_s$	0.49	0.63

TABLE 6 - Advantages and Disadvantages of the EDT test

ADVANTAGES		
Natural Delamination	Artificial Delamination	Both
No Inserts	with inserts	Configurations
*Easy to manufacture	*Well-defined delamination plane on edge	*Simple loading
*Distinct jump in load-displacement curve and delamination visible at onset	*E^* measured directly	*G independent of delamination size
*No size effect on G_c		*Several layups for range of mixed-mode conditions
*Delamination typical of those in structure		*Data consistent with other toughness tests
		*Provides ranking of Interlaminar Fracture Toughness of Composites

TABLE 6 (Continued)

DISADVANTAGES

Natural Delamination No Inserts	Artificial Delamination with inserts	Both Configurations
*Irregular Delamination forms on edge	*Requires Template to make panel	*G_c measurement limited by fiber failure
*E^* must be calculated	*E^* measurement affected by insert uniformity	*Non-linear behavior may occur before delamination onset
	*Delamination onset hard to detect	*No closed-form solution for G components
	*Some size effect on G_c	*Residual thermal and moisture stresses may influence G_c

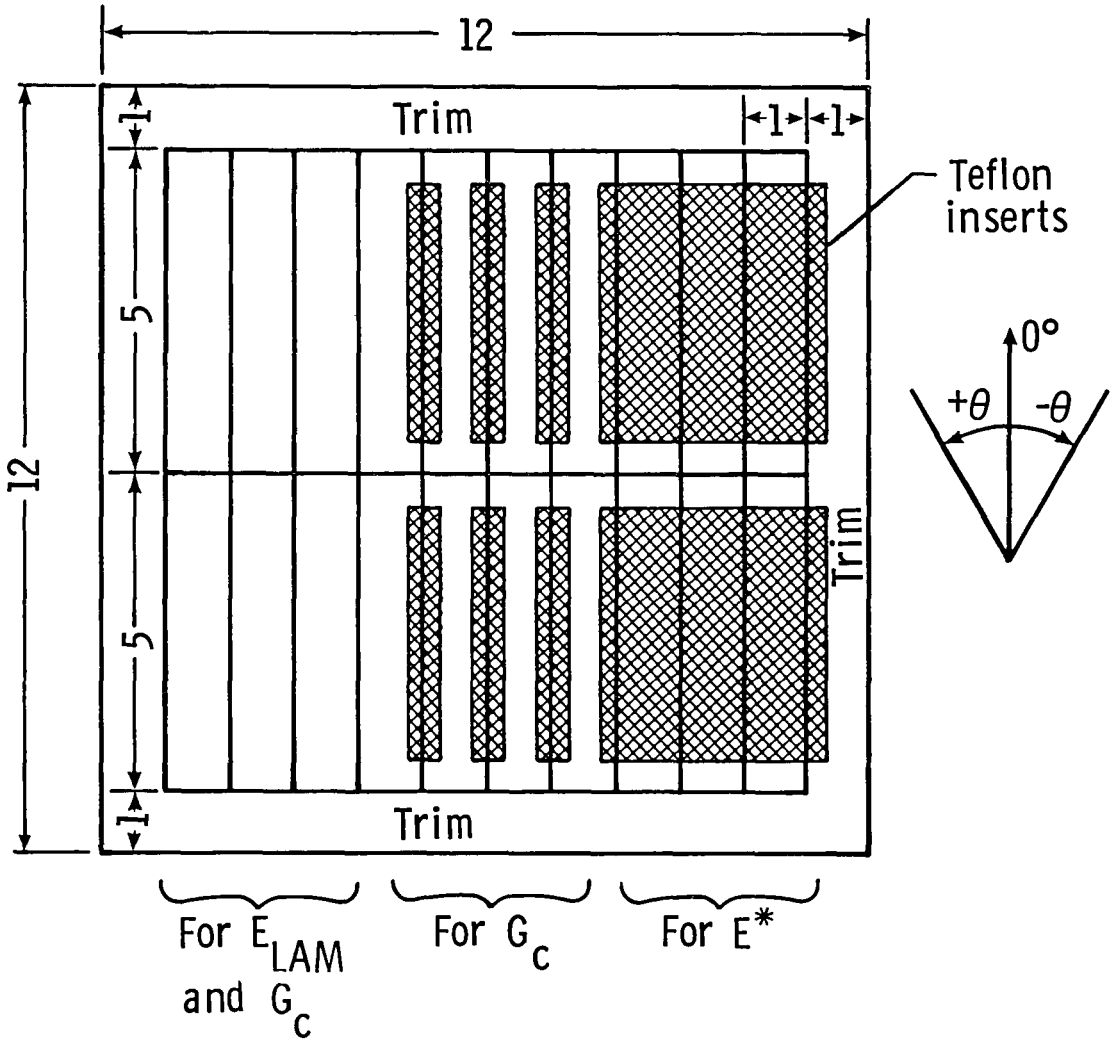

Fig. 1 EDT Panel Showing Coupon Location and Inserts (Dimensions Are In Inches)

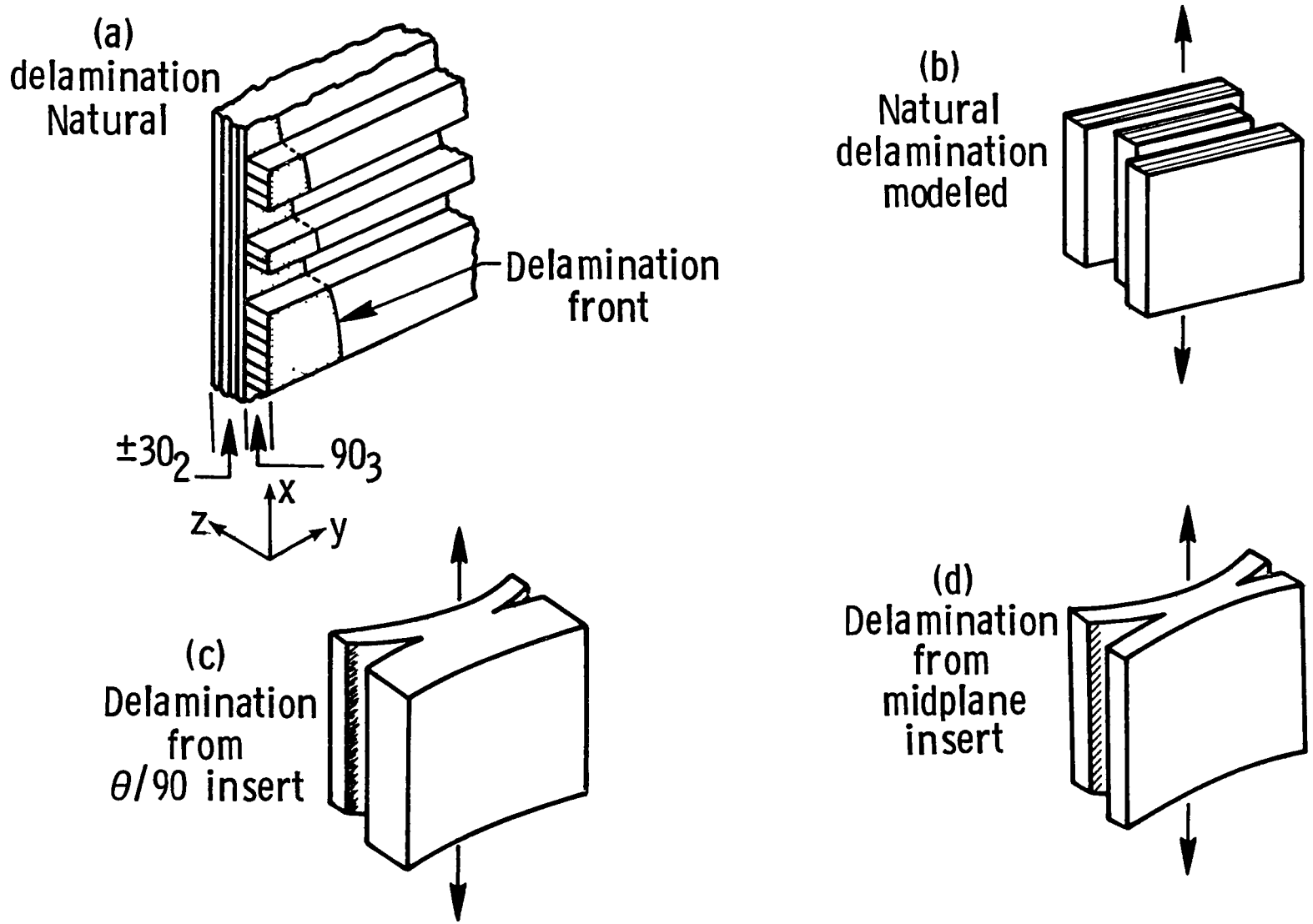

Fig. 2 EDT Test Configurations

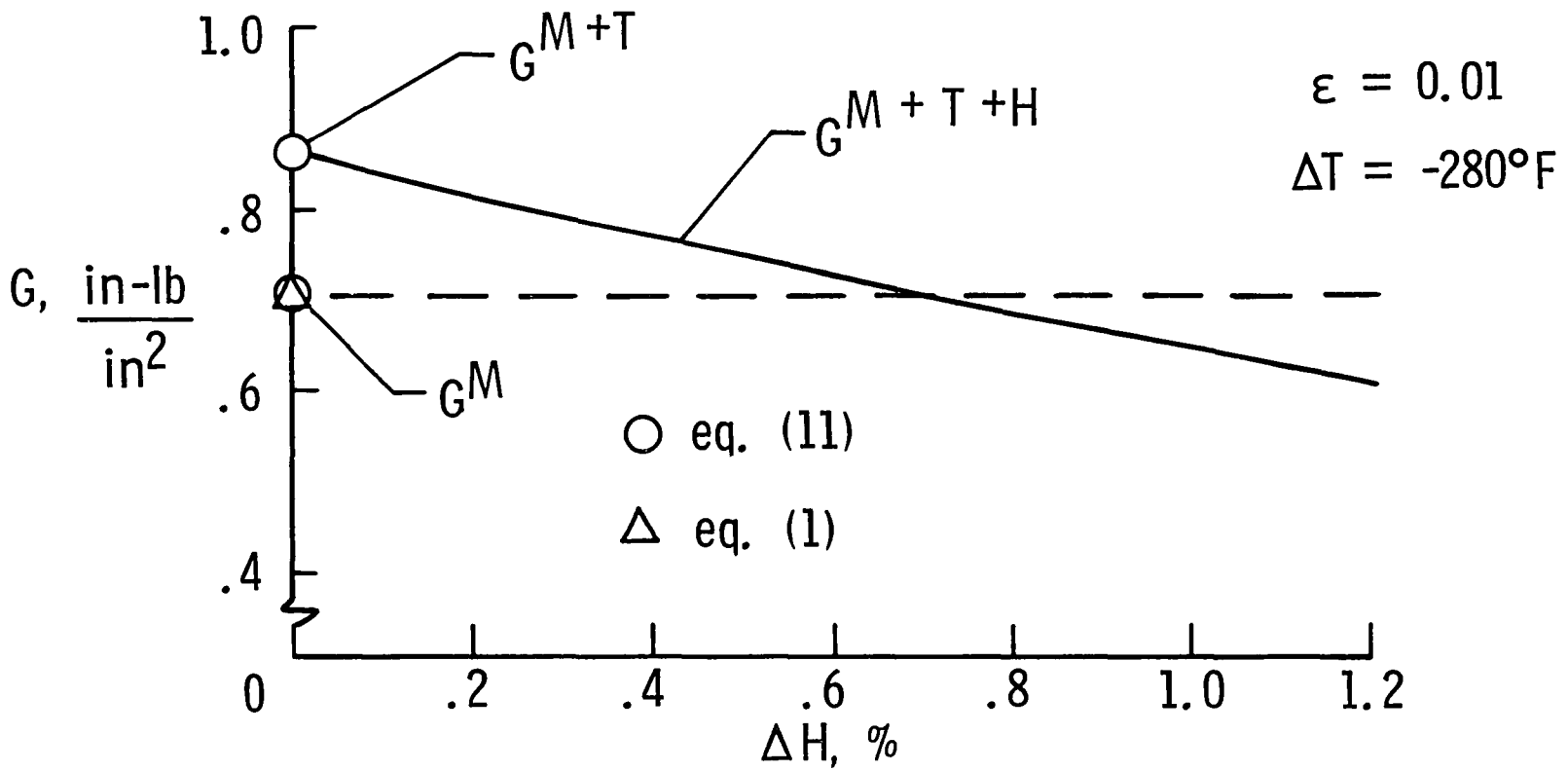

Fig. 3 Influence of Residual Thermal and Moisture Stresses on Strain Energy Release Rate

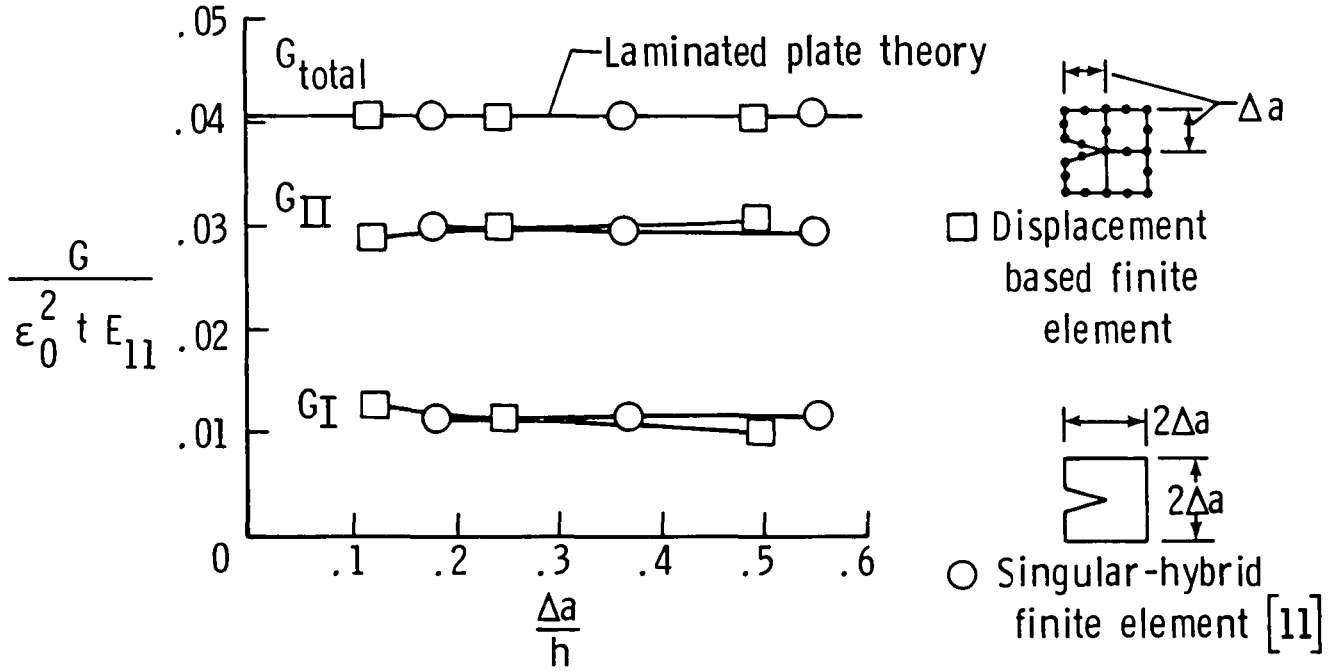

Fig. 4 Convergence Comparison for Displacement-Based and Singular-Hybrid Finite Element Analyses of $[0/\pm35/90]_s$ Laminates

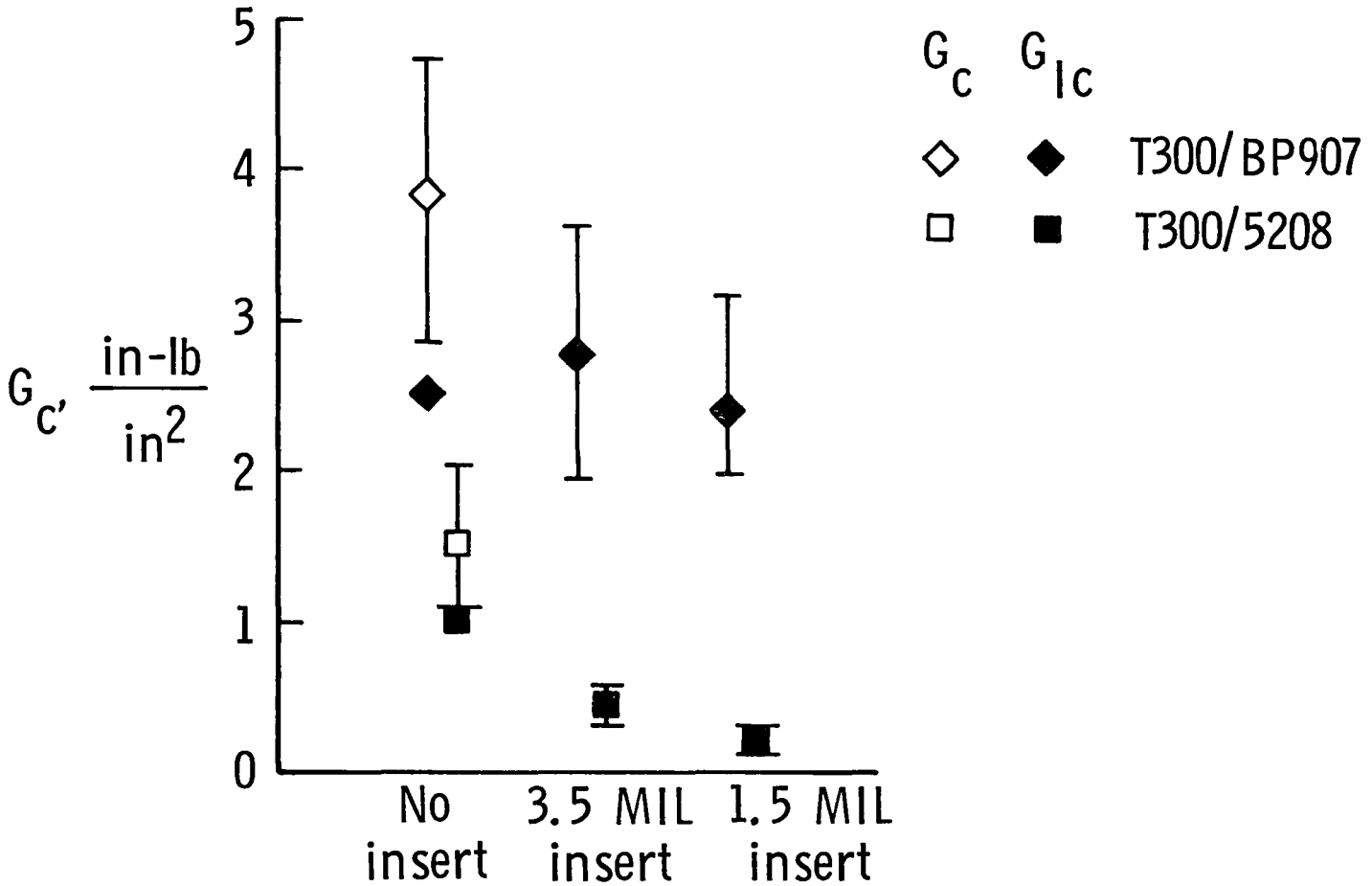

Fig. 5 Interlaminar Fracture Toughness From $[+30/-30_2/+30/90_2]_s$ EDT Tests With And Without Midplane Inserts

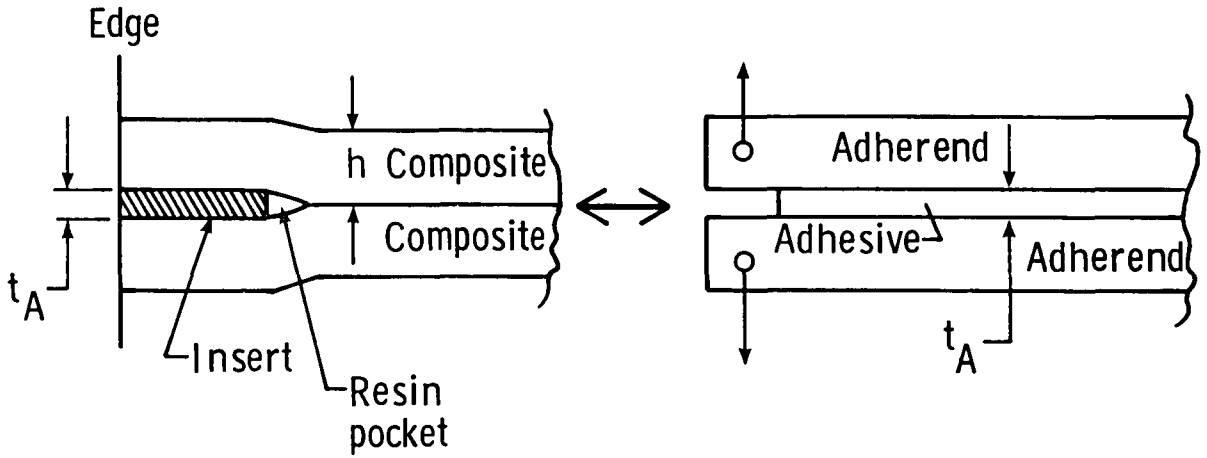

Fig. 6 Adhesive Bond Analogy For Delamination Growing From Insert

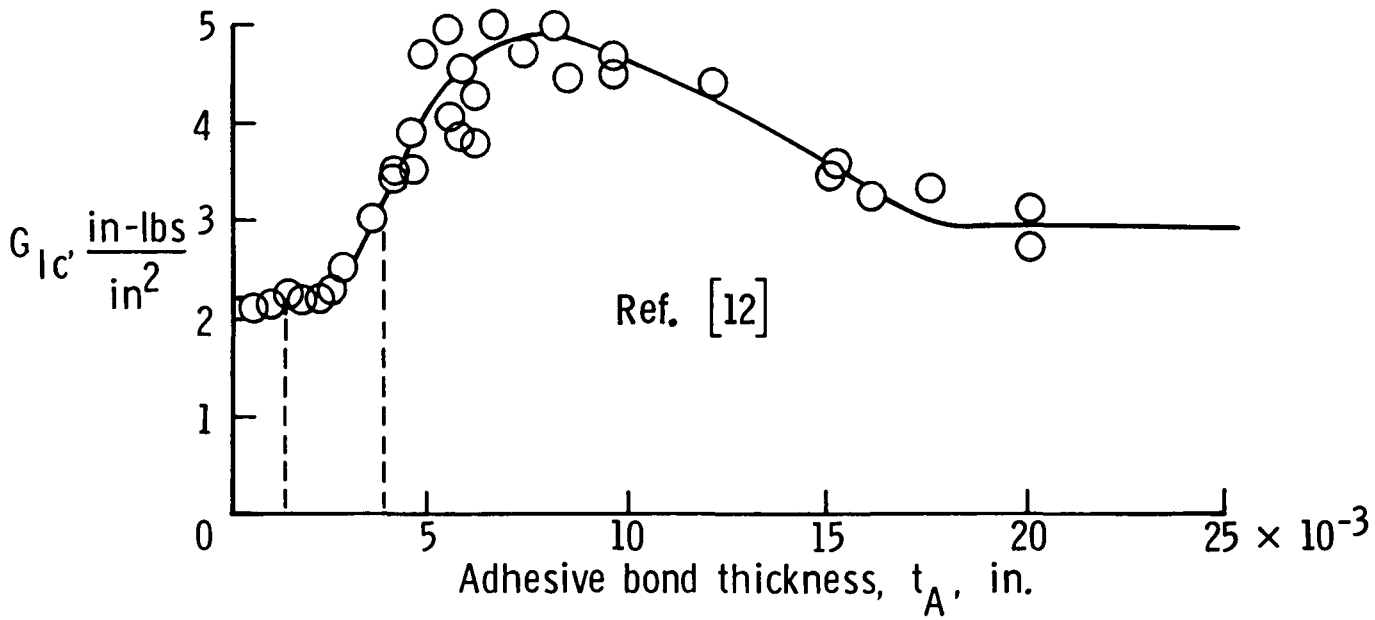

Fig. 7 Fracture Toughness as a Function of Bond Thickness for BP907 Adhesive in Double Cantilever Beam With Aluminum Adherends

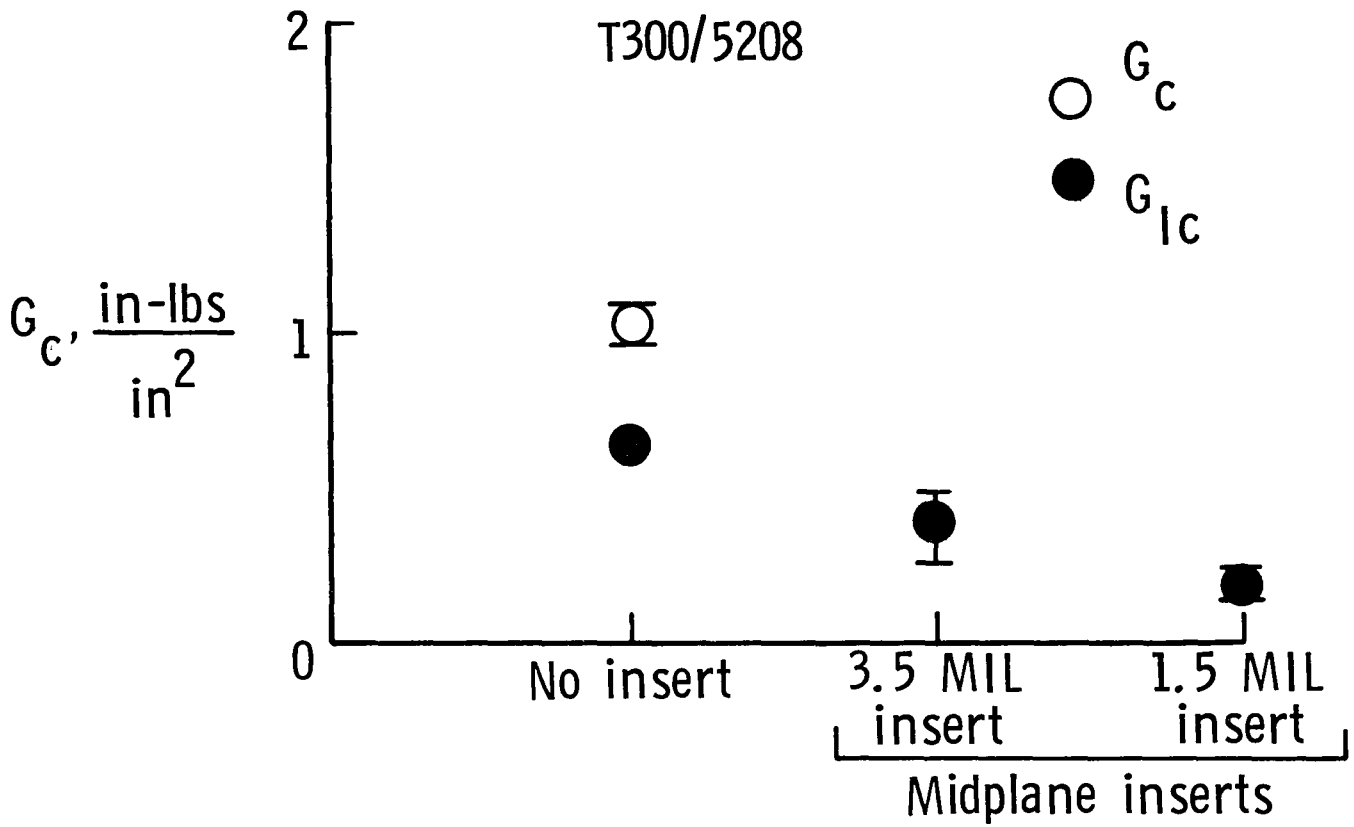

Fig. 8 Interlaminar Fracture Toughness From $[+30/-30_2/+30/90]_s$ EDT Tests

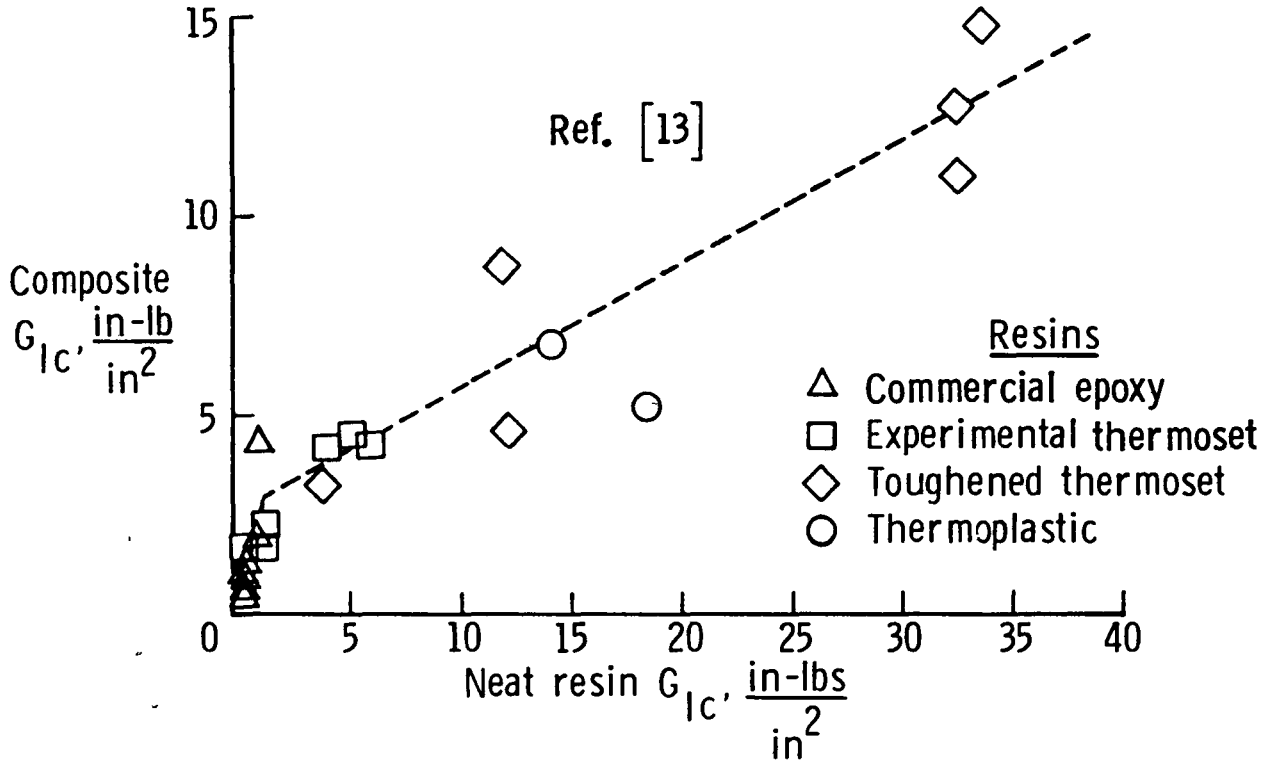

Fig. 9 Composite G_{Ic} Versus Neat Resin G_{Ic} For Various Resin Matrix Materials

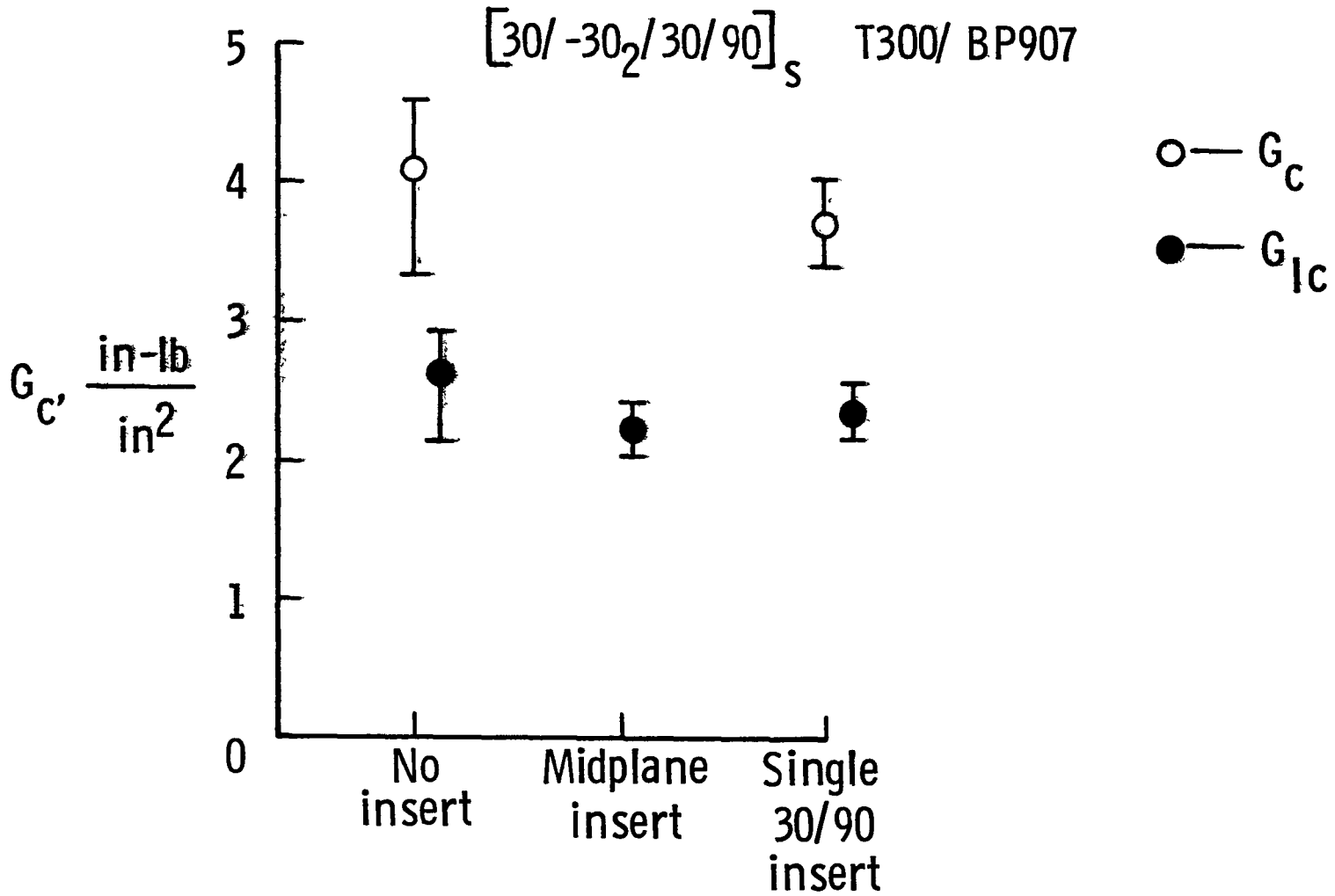

Fig. 10 Variation In G_c With Insert Location

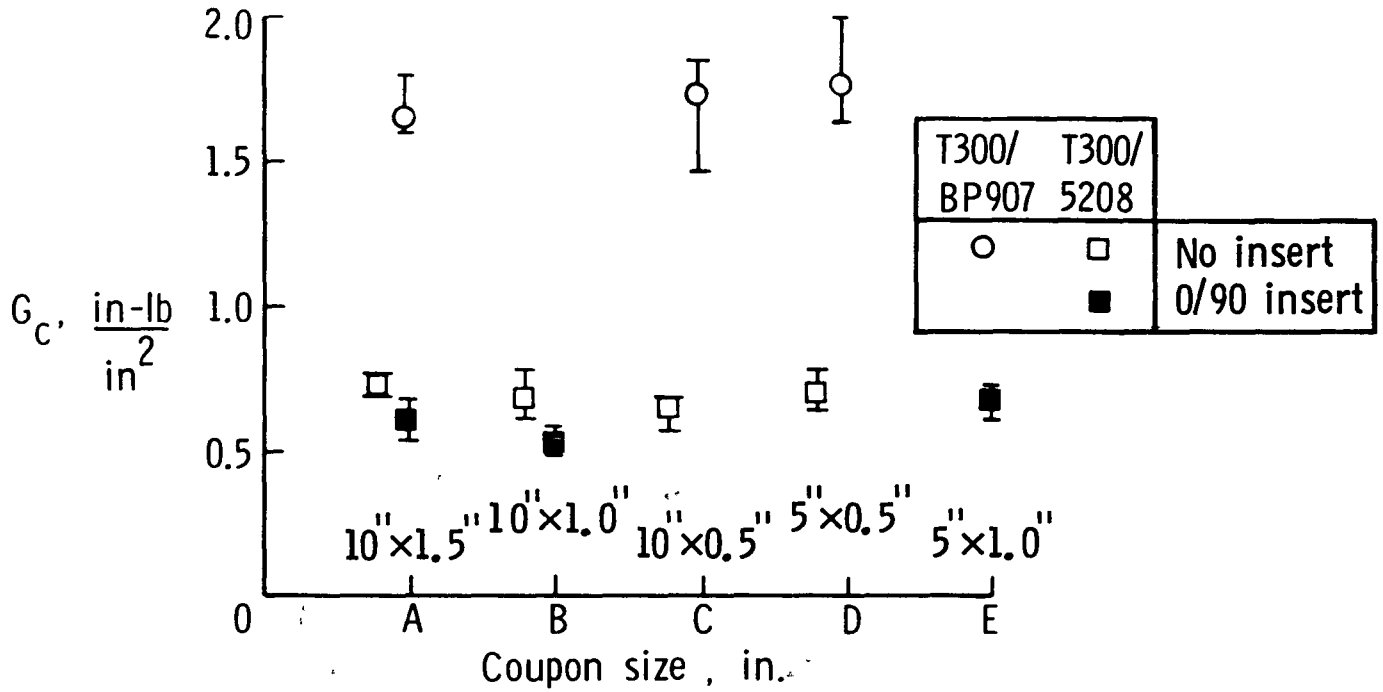

Fig. 11 Variation In G_c With Coupon Size For $(\pm 35/0/90)_s$ EDT Tests

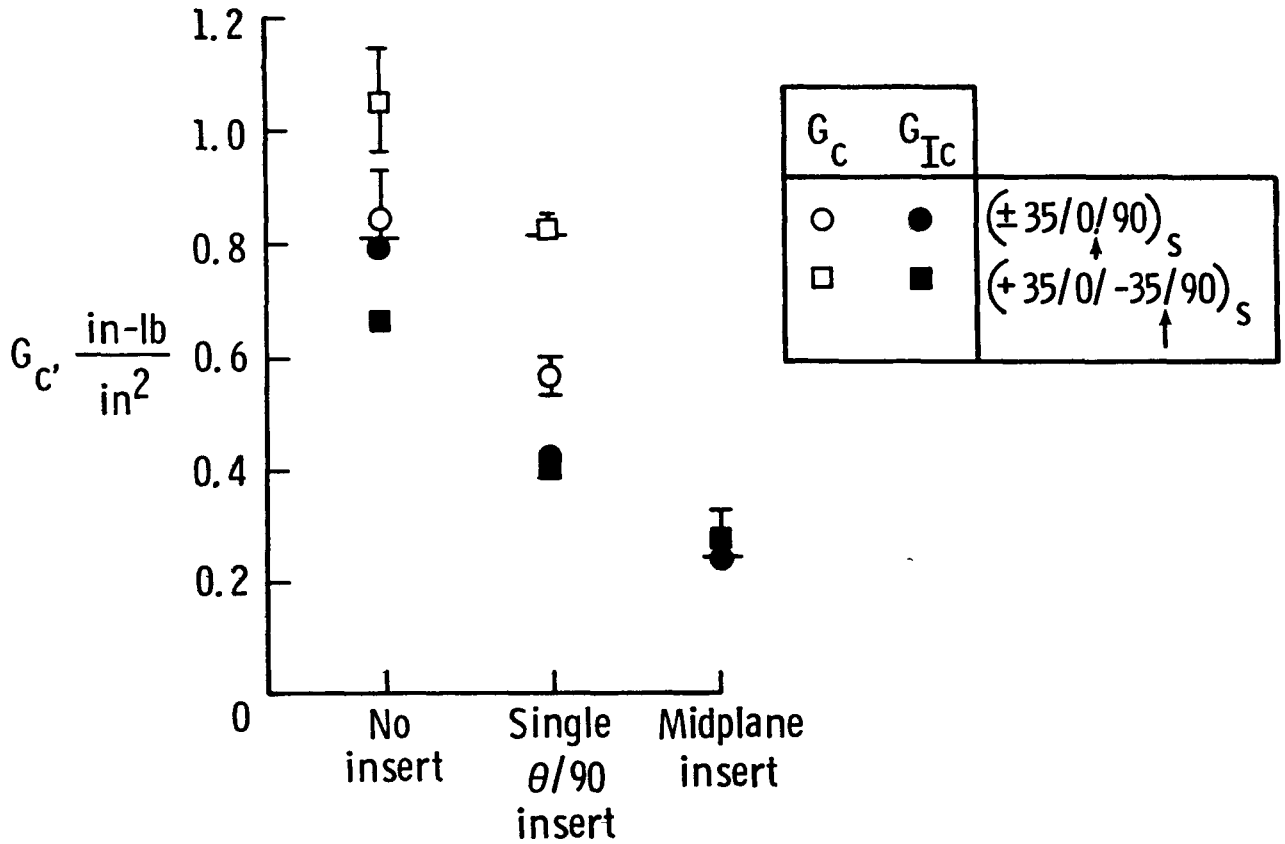

Fig. 12 Variation In G_c With EDT Layup And Configuration For T300/5208

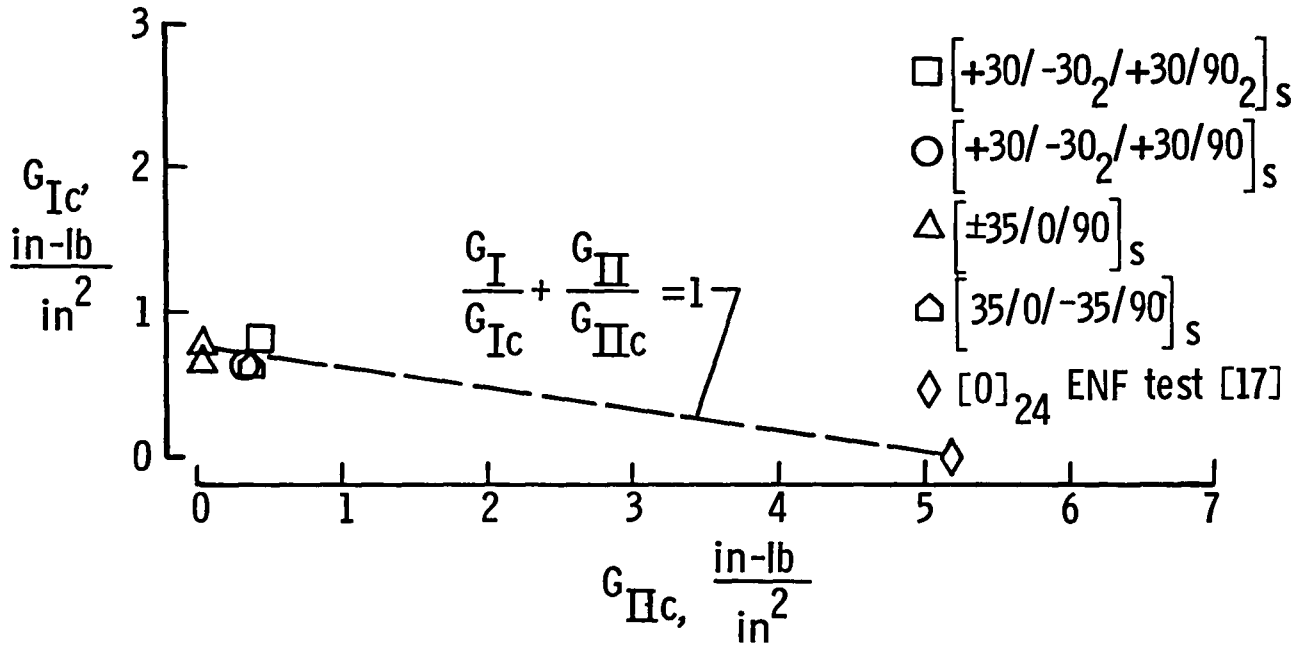

Fig. 13 Delamination Failure Criterion for T300/5208

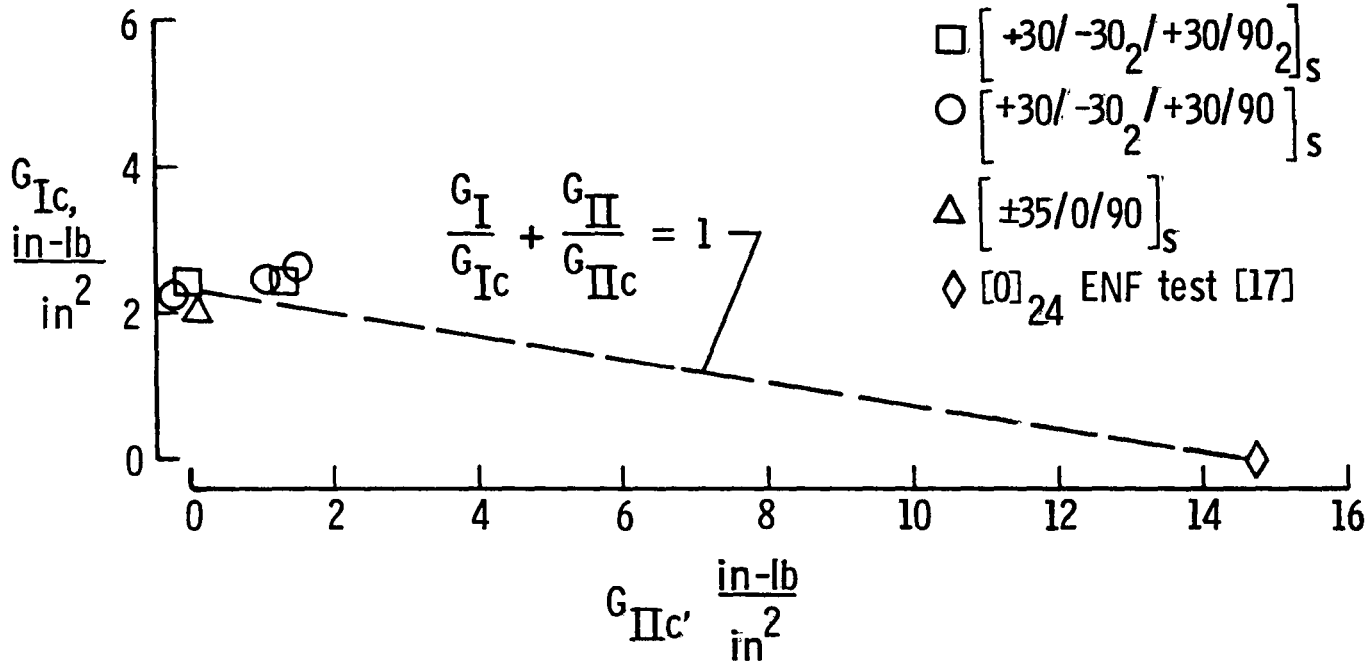

Fig. 14 Delamination Failure Criterion for T300/BP907

1 Report No	2 Government Accession No	3 Recipient's Catalog No
NASA TM-86433 USAAVSCOM TM 85-B-3		

4 Title and Subtitle	5 Report Date
Comparisons of Various Configurations of the Edge Delamination Test for Interlaminar Fracture Toughness	July 1985
	6 Performing Organization Code 534-06-23-03

7 Author(s)	8 Performing Organization Report No
T. K. O'Brien, N. J. Johnson and I. S. Raju	
	10 Work Unit No

9 Performing Organization Name and Address	11 Contract or Grant No
NASA Langley Research Center, Hampton, VA 23665 Structures Laboratory, USAAVSCOM Research & Technology Laboratories, Hampton, VA 23665	

12 Sponsoring Agency Name and Address	13 Type of Report and Period Covered
National Aeronautics and Space Administration Washington, DC 20546 and U.S. Army Aviation Systems Command St. Louis, MO 63166	Technical Memorandum
	14 Army Project No 1L161102AH45

15 Supplementary Notes

16 Abstract

Various configurations of Edge Delamination Tension (EDT) test specimens, of both brittle (T300/5208) and toughened-matrix (T300/BP907) graphite reinforced composite laminates, were manufactured and tested. The mixed-mode interlaminar fracture toughness, G_c, was measured using $(30/-30_2/30/90_n)_s$, n=1 or 2, $(35/-35/0/90)_s$, and $(35/0/-35/90)_s$ layups designed to delaminate at low tensile strains. Laminates were made without inserts so that delaminations would form naturally between the central 90° plies and the adjacent angle plies. Laminates were also made with Teflon inserts implanted between the 90° plies and the adjacent angle (θ) plies at the straight edge to obtain a planar fracture surface. In addition, interlaminar tension fracture toughness, G_{Ic}, was measured from laminates with the same layups but with inserts in the midplane, between the central 90° plies, at the straight edge. All of the EDT configurations were useful for ranking the delamination resistance of composites with different matrix resins. Furthermore, the variety of layups and configurations available yield interlaminar fracture toughness measurements needed to generate delamination failure criteria. The influence of insert thickness and location, and coupon size on G_c values were evaluated. For toughened-matrix composites, laminates with 1.5-mil thick inserts yielded interlaminar fracture toughness numbers consistent with data generated from laminates without inserts. Coupons of various sizes yielded similar G_c values. The influence of residual thermal and moisture stresses on calculated strain energy release rate for edge delamination was also reviewed.

17 Key Words (Suggested by Author(s))	18 Distribution Statement
composite materials, delamination, fracture, toughness, graphite epoxy	Unclassified - Unlimited Subject Category 24

19 Security Classif (of this report)	20 Security Classif (of this page)	21 No of Pages	22 Price*
Unclassified	Unclassified	49	A03

*For sale by the National Technical Information Service, Springfield, Virginia 22161

End of Document